The official journal of
INTERNATIONAL FEDERATION OF PIGMENT CELL SOCIETIES · SOCIETY FOR MELANOMA RESEARCH

PIGMENT CELL & MELANOMA Research

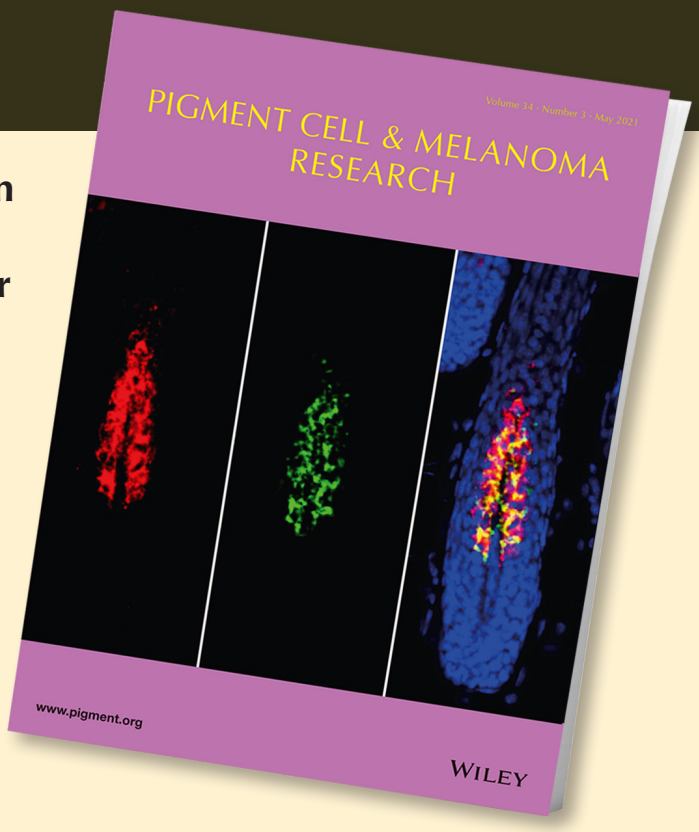

Transcriptomic analysis and *ednrb* expression in cochlear intermediate cells reveal developmental differences between inner ear and skin melanocytes

Justine M. Renauld | William Davis | Tiantian Cai | Claudia Cabrera | Martin L. Basch

DOI: 10.1111/pcmr.12961
Volume 34, Issue 3, Pages 585–597

Received: 24 September 2020 | Revised: 29 December 2020 | Accepted: 16 January 2021

DOI: 10.1111/pcmr.12961

ORIGINAL ARTICLE

WILEY

Transcriptomic analysis and *ednrb* expression in cochlear intermediate cells reveal developmental differences between inner ear and skin melanocytes

Justine M. Renauld[1] | William Davis[1] | Tiantian Cai[2] | Claudia Cabrera[3] | Martin L. Basch[1,3,4,5]

[1]Department of Otolaryngology, Head & Neck Surgery, Case Western Reserve University School of Medicine, Cleveland, OH, USA

[2]Program in Developmental Biology, Baylor College of Medicine, Houston, TX, USA

[3]Department of Otolaryngology, Head & Neck Surgery, University Hospitals, Cleveland, OH, USA

[4]Department of Genetics and Genome Sciences, Case Western Reserve School of Medicine, Cleveland, OH, USA

[5]Department of Biology, Case Western Reserve School of Medicine, Cleveland, OH, USA

Correspondence
Martin L. Basch, Department of Biology, Case Western Reserve School of Medicine, Cleveland, OH, USA.
Email: mlb202@case.edu

Funding information
Hearing Health Foundation, Grant/Award Number: emerging research grant; National Institute on Deafness and Other Communication Disorders, Grant/Award Number: 1 R01 DC015785-01

Abstract

In the inner ear, the neural crest gives rise to the glia of the VIII ganglion and two types of melanocytic cells: The pigmented cells of the vestibular system and intermediate cells of the stria vascularis. We analyzed the transcriptome of neonatal intermediate cells in an effort to better understand the development of the stria vascularis. We found that the expression of endothelin receptor B, which is essential for melanocyte development, persists in intermediate cells long after birth. In contrast, skin melanocytes rapidly downregulate the expression of *EdnrB*. Our findings suggest that endothelins might have co-opted new functions in the inner ear during evolution of the auditory organ.

KEYWORDS

cochlea, development, *EdnrB*, intermediate cells, melanocytes, stria vascularis

1 | INTRODUCTION

The neural crest is an embryonic transient cell population specific to vertebrates that originates in the dorsal neural tube. Around the time of neural tube closure, neural crest cells undergo an epithelial-to-mesenchymal transition and migrate extensively in the embryo to give rise to a wide variety of derivatives. These include most of the craniofacial skeleton, neurons, and glia of the peripheral nervous system, and all the pigmented cells in the body (Basch & Bronner-Fraser, 2006; Prasad et al., 2019). Among the neural crest cell derivatives, the melanocytes are defined as dendritic pigmented cells producing melanin (Ali & Naaz, 2015). In mammals, melanocytes are differentiated into two populations, the cutaneous that are KIT-sensitive, and the extra-cutaneous or non-classical melanocytes and dermal melanocytes, which are less sensitive to KIT signaling (Aoki et al., 2009). The first category is present in the skin where they participate in the pigmentation of the epidermis and hair follicles. The second category can be found in different locations of

the body such as the nervous system, heart, eye, and inner ear (Ali & Naaz, 2015; Vandamme & Berx, 2019). After birth, most skin melanocytes and their precursors will remain in the hair follicle (Djian-Zaouche et al., 2012) except for a few regions such as the pinna, foot, and tail, which present many extra-follicular epidermal melanocytes and dermal melanocytes (Fitch et al., 2003). The mouse tail's skin is a good model for human skin pigmentation because of the few follicular melanocytes and many extra-follicular epidermal melanocytes, which makes it similar in composition to the human skin (Tharmarajah et al., 2018).

Neural crest and melanocyte lineage studies have shown that melanoblasts begin migration around E9, and they reach the epidermis where they proliferate at E12.5-E13.5 (Shin et al., 1999; Yoshida et al., 1996). Once in the epidermis, melanoblasts progressively accumulate in the forming hair follicles. In contrast to the skin, neural crest cells migrate into the developing otocyst around E9.5 and by E12.5 they form the glia of the cochleovestibular ganglion and the pigmented cells of the vestibular organs. Around E15.5, melanoblasts also begin ingressing in the lateral wall of the cochlea to form the intermediate cells of the stria vascularis (Ohyama, 2017; Shibata et al., 2016). It is still unclear whether the Schwann cell precursors, which have the potential to differentiate into melanoblasts, give rise to glia, melanocytes of the vestibular system, and intermediate cells, or whether these originate from different subpopulations of migratory neural crest (Furlan & Adameyko, 2018).

The stria vascularis is a specialized epithelium localized in the lateral wall of the mammalian cochlea. It is responsible for the production of endolymph, a low sodium and high potassium fluid that fills the scala media, generating a positive endocochlear potential. The endocochlear potential generated by the endolymph is the driving force that allows mechanosensory hair cells to transduce the sound input into nerve impulses (reviewed in Casale & Agarwal, 2020; Nin et al., 2016). Melanocyte-like intermediate cells are essential for strial function (Steel & Barkway, 1989). Mutations that affect neural crest development or migration as well as melanocyte differentiation can result in sensorineural hearing loss.

The endothelin family of signaling molecules is composed of two G protein-coupled transmembrane receptors (EDNRA and EDNRB) and three ligands (EDN or ET-1, ET-2, ET-3) (Sakurai et al., 1990). This family has been first studied for its implication in vasoconstriction and vascular disease research (reviewed in Davenport et al., 2016). In mice, spontaneous mutations in the endothelin receptor B locus result in piebaldism, while in humans it causes the Waardenburg syndrome (Matsushima et al., 2014; Tachibana et al., 2003). In both cases, in addition to an aganglionic megacolon, the skin and the inner ear are missing melanocytes, which result in pigmentation defects and in strial deafness (Ni et al., 2013; Waardenburg, 1951). The essential role played by the couple EDNRB/EDN3 in the normal development of melanocytes and enteric ganglion neurons was corroborated over two decades ago using knockout mouse models (Baynash et al., 1994; Hosoda et al., 1994). These conditional knockout mice lack the *EdnrB* receptor in neural crest cells and phenocopy the piebald mutation (Druckenbrod et al., 2008). Studies using the TetO system suggest that *EdnrB* is transiently required for melanoblast development only between E10.5 and E12.5 (Shin et al., 1999). It has been proposed that *EdnrB* is essential in promoting the proper migration of melanoblasts at early stages rather than mediating their fate specification (Lee et al., 2003; Osawa, 2008). In fact, adult skin melanocytes do not express *EdnrB* unless after a skin lesion or during melanoma progression (Demunter et al., 2001).

SIGNIFICANCE

Endothelin signaling is necessary for melanocyte development. *EdnrB* expression is quickly downregulated in skin melanocytes after they reach the hair follicle and is only upregulated after skin lesions or melanoma progression. In the inner ear, we found sustained expression of *EdnrB* in cochlear melanocytes, suggesting new roles for this signaling pathway acquired during evolution of the auditory organ. Our findings could have implications in melanocyte biology and melanoma.

In contrast, cochlear melanoblasts do not fully differentiate into mature intermediate cells of the stria vascularis until approximately 12 days after birth (Ohyama, 2017; Shibata et al., 2016; Steel & Barkway, 1989). During this time, neural crest cells migrate to their final position between the marginal and basal cells, dramatically change their morphology to become elongated at first, and then develop interdigitations to establish tight junctions with the other cell layers of the stria (Cable et al., 1992). In addition, they become intimately associated with the blood capillaries that invade the stria from the spiral ligament plexus (Shi, 2016). Endothelin signaling has been implicated in all the processes that occur during intermediate cell differentiation, such as migration, proliferation, angiogenesis, vasculogenesis, and cytoskeletal rearrangement (Maguire & Davenport, 2015; Saldana-Caboverde & Kos, 2010). Here, we report persistence of *EdnrB* expression in cochlear melanocytes after birth. We hypothesize that a differential expression of *EdnrB* between skin melanocytes and intermediate cells could suggest multiple roles for *EdnrB* in the development of the stria vascularis.

2 | MATERIALS AND METHODS

2.1 | Experimental animals

Wnt1-Cre2 (129S4.Cg-*E2f1*$^{Tg(Wnt1\text{-}cre)2Sor}$/J) and Ai3 (B6.Cg-Gt(ROSA)26Sortm32(CAG-COP4*H134R/EYFP)Hze/J mice were used to generate Wnt1 reporter embryos. For in situ hybridizations and immunohistochemistry, we used C57Bl/6 mice. All lines were obtained from Jackson Laboratories and bred in our animal facility in compliance with the Case Western Reserve University Institutional

Animal Care and Use Committee (IACUC Protocol 2018–0034). C57Bl/6 mice were sacrificed at different time points from embryonic day 11 (E11) to post-natal day 90 (P90). The cochleae were dissected with two forceps under a stereomicroscope after CO_2 euthanasia.

The cochleae were fixed in 4% paraformaldehyde in PBS overnight at 4°C. After washes in PBS, the post-natal cochleae were decalcified at 4°C in EDTA (0.5 M) in PBS as long as necessary. The samples were then washed several times in PBS and incubated at 4°C in 30% (w/v) sucrose in PBS until the cochleae sank in the tube. The cochleae were embedded in OCT and stored at −80°C. The cryosections (12–16 μm thick) were obtained by a cryostat (Microm).

2.2 | Cell dissociation and FACS

We generated pups where all neural crest derivatives are labeled with EYFP by crossing Wnt1-Cre mice to Ai3 reporters (Lewis et al., 2013). We collected inner ears from these pups at post-natal day 1 in CMF PBS. The lateral wall of the cochleae was dissected and collected in 1.5-ml tubes. The tissue was treated with 0.1% trypsin and 0.5 mM EDTA in CMF PBS for 10 min at 37°C and then washed in CMF PBS + DMEM and FBS to inactivate the trypsin. The cells were dissociated by gently pipetting on ice and filtered with a cell strainer cap (BD Biosciences). The dissociated and filtered cells were sorted in a FACSAria II Cell Sorter (BD Biosciences) at 4°C in PBS containing 2% FBS, using a 130-μm nozzle. The cells were collected on the basis of their fluorescence gating in DMEM 5% FBS, spun down, lysed in RTL buffer (Qiagen), and stored at −80°C. Between 10,000 and 180,000 sorted cells from freshly dissected cochleae were collected to make libraries for RNAseq. The identity of sorted cells was confirmed using epifluorescence.

2.3 | RNA sequencing

For RNAseq libraries, total RNA from $EYFP^+$ and $EYFP^-$ sorted cells was extracted as previously described (Maas et al 2,106). Duplicate libraries for each condition were prepared from a total of 10,000–180,000 cells yielding approximately between 250 and 450ng of RNA. The libraries were generated using RNAseq TruSeq RNA Sample Preparation Kit v2 (Illumina) according to manufacturer's instructions. Quality, quantity, and integrity of the libraries were obtained by electrophenogram in an Agilent Bioanalyzer. Pair-end sequencing was performed in HiSeq 200 Sequencing Platform (Illumina). Bioinformatic analysis of the reads was done using TopHat1.4.1 software, and the number of reads per gene and per library was obtained using DESeq program. Reads were aligned to the Mus musculus Ensembl mm9 iGenome (Illumina). In order to find genes enriched in intermediate cells, a significantly DEG was considered to have a reads per kilobase million of transcripts (RPKM) higher than 3,000, fold change (FC) higher than 4, and value and FDR < 0.01. The files generated have been deposited in the NCBI GEO database, Accession No. GSE14275.

2.4 | Gene ontology analysis

We uploaded our list of differentially expressed genes to the Gene Ontology enRIchment anaLysis and visuaLizAtion tool (Gorilla) website (http://cbl-gorilla.cs.technion.ac.il) to cluster the intermediate cell genes according to biological process, metabolic function, and regulation of biological process. We conducted similar analyses using the Gene Ontology Resource and Panther Classification System (http://geneontology.org).

2.5 | RNA probe synthesis and in situ hybridization

Digoxigenin-labeled antisense riboprobes were synthesized as previously described (Stern et al., 1998). Briefly, mouse genomic DNA templates were used to synthesize each probe by PCR with digoxigenin-labeled NTPs, and forward and reverse primers in which the T7 RNA polymerase sequences were included in the reverse primer (probes sequences in Table S1).

In situ hybridization was performed as already described previously (Maass et al., 2016). Slides were incubated in DEPC-PBS for 10 min, twice. For post-natal stages, the slides were incubated in proteinase K solution (1.6 μg/ml) for 5 min, rinse 3 times for 5 min in DEPC-PBS, and then fixed in 4% paraformaldehyde in DEPC-PBS for 10 min followed by 3 rinses of 5 min in DEPC-PBS. The slides were incubated in acetylation buffer (0.25% acetic anhydride in 0.1M triethanolamine, pH 8.0) for 10 min and rinsed 3 times for 5 min in DEPC-PBS. The sections were incubated in hybridization buffer (50% Formamide; 5X SSC, 5X Denhardts, 250 μg/ml yeast RNA) (Sigma R6750) and 100 μg/ml salmon sperm DNA (Invitrogen 15,632,011) for 30 min at 65°C. The slides were incubated in hybridization buffer containing the DIG-labeled probes (1mg/ml) covered with glass coverslips overnight at 65°C. The next day, coverslips were removed and the slides were washed for 10 min in 0.2X SSC at 65°C, followed by two more wash for 20 min each in 0.2x SSC at 65°C. Slides were then washed at room temperature for 5 min in PTw (0.1% Tween 20 in PBS) and then blocked for at least 30 min in PTw with 10% serum and 0.2% Na azide. Slides were stained for 1 hr in PTw containing 10% serum with 1:2000 anti-digoxygenin alkaline phosphatase antibody. The slides were washed three times in PTw for 5 min each and then incubated for 10 min in alkaline phosphatase buffer (100 mM Tris, pH 9.5, 50 mM $MgCl_2$, 100 mM NaCl, 0.1% Tween 20). The slides were then developed in an alkaline phosphatase buffer containing 0.33 mg/ml of NTB and 0.18 mg/ml of BCIP protected from light. The slides were observed under a microscope until the desired staining was observed. The reaction was stopped by washing the slides in PBS 3 times for 5 min and fixed with 4% paraformaldehyde in PBS, pH 7.2, for 20 min. The slides were finally rinsed in PBS and mounted with a coverslip and Fluoromount.

2.6 | RNAscope in situ hybridization and immunohistochemistry

RNAscope for *EdnrB* mRNA was performed on frozen sections using the RNAscope Multiplex Fluorescent Reagent Kit v2 (Cat. No. 323,136). The in situ hybridization was performed according to the manufacturer's instructions with a positive control probe mixture (including 3 housekeeping genes, *Polr2a*, *Ppib*, and *Ubc*), a negative control probe (*DapB*), and Mm-*EdnrB* probe (473,801). Briefly, the slides were washed with 1X PBS and then dried at 60°C for 30 min. The slides were post-fix by immersing them in 4% paraformaldehyde in 1X PBS for 15 min at 4°C. The dry slides were incubated with RNAscope® hydrogen peroxide for 10 min at RT and then rinsed in distilled water. The sections were boiled in RNAscope® 1X Target Retrieval Reagent for 10 min. The sections were rinsed in distilled water, transferred into 100% alcohol for 3 min, and then dry at RT for 5 min. A hydrophobic barrier pen was used around each section before the next steps. The sections were incubated in RNAscope® Protease III during 20 min at 40°C followed by 3 rinses in distilled water. The slides were incubated with the respective probes during 2 hr at 40°C, followed by 3 wash in the washing buffer. The slides were put in contact with the amplification reagent AMP1, AMP2, and AMP3 for 30, 30, and 15 min, respectively, separated by a wash in the washing buffer between each step. The sections were incubated in the HRP-C1 reagent for 15 min at 40°C followed by wash in washing buffer and incubation with the Opal 570 solution (1/1,000, FP1488A—Akoya Biosciences) for 30 min at 40°C before been blocked with the HRP blocker for 15 more minutes. After this RNAscope protocol, the sections were directly used for immunostaining as follows. The sections were rinsed in PBS and blocked in PGT (PBS—0.25% gelatin and 0.3% Triton X-100) for 30 min. The sections were incubated with the primary antibody solution diluted in PGT overnight at 4°C (rat anti-CD44(H-CAM)—1/250—MA4405, Thermo Fisher Scientific; rabbit anti-DCT/TRP2—1/100—ab74073, Abcam; chicken anti-GFP—1/100—ab13970, Abcam). The sections were washed 3 times in PBS and incubated for 1 hr at RT with the secondary antibody diluted in PBS (Alexa 488 donkey anti-rat—1/1000—A21208; Thermo Fisher Scientific; Alexa 633 goat anti-rabbit—1/1000—A21070, Thermo Fisher Scientific; Alexa 488 goat anti-chicken—1/1000—A11039, Thermo Fisher Scientific). Finally, the sections were rinsed in PBS and mounted with Fluoromount.

To insure the proper functioning of the RNAscope, the positive control and the DapB-negative control were analyzed in parallel to the stages to confidently make a call on the expression of our target RNA in the tissue specimen. After discussion with the company, we decided to normalize our score for the ear post-natal stage to take into account the hardship of the decalcification. The positive and negative controls were performed on adjacent slides (each inner ear was cut and placed on a series of 5 slides where each section was placed on each slide before restarting at slide number 1 to have comparable slides).

The normalization was performed as discussed with the Technical Support Scientist for Advanced Cell Diagnostics. We used the 3 plex-positive control probe data to do so as recommended by the company to take into consideration the decalcification process. Positive control genes are understood to be present in constant abundance in all samples. The difference in positive control expression was used to normalize the expression of our gene of interest (each sample was divided by the ratio of his positive control value compared with P0 (e.g., if our positive control was 3 times less expressed at P15 than at P0, the expressions of our gene of interest at P15 would be multiplied 3 times before comparing it within both stages).

The scoring of the number of dots/cell was performed as it is the data analysis method recommended by the company to assess the expression of an mRNA per cell (the number of cells of interest can vary widely between samples, and it is then more accurate to divide them by the number of cells analyzed by section to assess the expression of our gene of interest per cell).

The slides were examined under an Apotome microscope using a 60x objective.

2.7 | Statistical analysis

After ratios were calculated at stages E11, E16.5, P0, P6, P15, and at 3 monthsomparisons of the ratios were performed between all stages. Additional comparisons were made for the r,atios between ear and skin at stages E16.5, P0, P6, P15, and at 3 months.

Analyses of the data revealed non-normal distribution. The Wilcoxon tests were used to perform comparisons between two groups, and the Kruskal–Wallis tests were used to assess comparisons between multiple groups. Significance was considered at $\alpha < 0.05$. All analyses were made using R 3.5.6.

Note from company: Score reliable when the UBC-positive control has a score of 3+/4+ (POLR2A 1+) and the *DapB*-negative control has a score of 0/1+, you can confidently make a call on the expression of your target RNA in the tissue specimen.

3 | RESULTS

3.1 | Neonatal transcriptomic analysis suggests a transitional state for intermediate cells of the stria vascularis

Intermediate cells of the stria are not derived from the otic placode unlike most cell types in the inner ear. They are melanocytic cells derived from the neural crest. They ingress into the lateral wall of the cochlea starting at around E14.5, and they complete this process around birth. To better understand the molecular cues that guide this process, we analyzed the transcriptome of intermediate cells a day after birth. The isolation and sequencing of mRNA from intermediate cells are summarized in Figure 1.

From a total of 4,921 differentially expressed genes identified by Ensembl ID, we found 2084 genes upregulated twofold or more

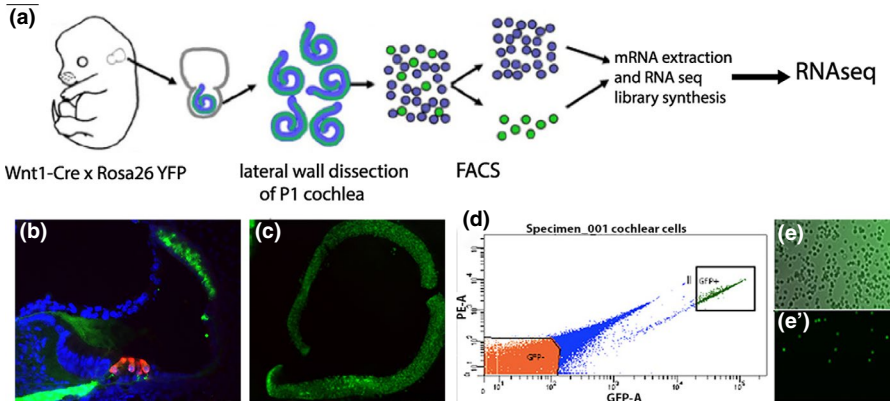

FIGURE 1 RNAseq of intermediate cells of the stria vascularis at P1. a. Experimental design. b. Section of a P1 cochlea from a Wnt1-Cre x Ai3 reporter mouse, which was used in the experiment. c. Dissected lateral wall of the cochlea shown in b. d. FACS report showing the purity of the EYFP + cells. e, e′. bright field and fluorescence fields of the sorted intermediate cells

and 2,826 genes downregulated twofold or more in the intermediate cell population compared with the other cell types in the inner ear, with a false discovery rate < 0.01. Table 1 shows a selection of the most upregulated and downregulated genes in intermediate cells. The complete list of differentially expressed genes is given in Table S2. Genes that are highly expressed not only in intermediate cells but also in marginal and basal cells are not represented in our list.

Many of the genes highly enriched in intermediate cells at postnatal day 1 such as *Tyrp1*, *Tyr*, and *Slc45a2* belong to the melanin synthesis pathway, suggesting that the neural crest that gave rise to these cells has started to differentiate to a melanocyte-like fate. However, we also found many genes that are expressed by undifferentiated neural crest, including *FoxD3*, which is known to suppress the melanocytic pathway. Since intermediate cells do not fully differentiate morphologically or functionally until P14, our results suggest that at neonatal stages their transcriptome reflects a transitional state between neural crest cells and mature intermediate cells. To confirm these data, we performed a gene ontology analysis, which revealed that, indeed, the neonatal intermediate cell transcriptome is enriched with general neural crest genes and with specialized melanoblast transcripts such as those involved in melanin biosynthesis and melanocyte differentiation (Figure S1).

3.2 | Validation of the RNAseq screen

Previous studies that used in situ hybridization to validate hair cell-specific transcripts found that only about 50% of hair cell-enriched transcripts gave detectable, hair cell-specific expression patterns (Cai et al., 2015). Therefore, to further validate the expression of our selected genes, we examined the expression of selected genes on cochlear sections of P1 mice by in situ hybridization (Figure 2). We chose genes on the basis of their RPKM values, significant enrichment, and potential functional role in the differentiation of the stria vascularis. In some cases where we identified signaling pathways, we also tested other components of the pathways (receptor, ligands, and downstream effectors) in order to better understand the cellular interactions during strial development. A sample of our results is shown in Figure 2. Only in a few cases did we see specific expression of the transcripts restricted to intermediate cells (*Tyrp1*, *Gsta4*, *EdnrB*). In other cases, transcripts were expressed in intermediate cells and marginal or basal cells (*Sema4a*, *Plexin1*, *Cxcr3*, *Rasgpr3*). Because in situ hybridization yields only spatial information, we cannot speculate about the differences in expression levels of transcripts present in multiple cell types.

3.3 | Cochlear versus skin melanoblasts

Previous research has identified genes with unique roles in cochlear melanocytes (Uehara et al., 2009). To further understand the differences between skin and inner ear melanocytes, we compared the transcriptome of P1 intermediate cells of the stria vascularis with a data set from E17.5 mouse skin melanoblasts (Marie et al., 2020). Although there is a slight discrepancy in the age of the melanoblasts we are comparing (E17.5 versus P1), skin melanocytes reach their target tissue and commence their differentiation a few days earlier than intermediate cells in the ear (Ohyama, 2017; Shin et al., 1999).

We compared all the genes upregulated in intermediate cells with the transcriptome of E17.5 skin melanoblasts. We identified 232 genes that are present in the cochlear but not skin melanoblasts (Table S3). 166 genes are predicted or unannotated sequences. The remaining 66 genes can be divided into four main categories: metabolic function (*Enho*, *Leprel1*, *Tmem195*, *Lass6*, *Il28ra*, *Mobkl1a*), ion channels (*Tmem20*, *Clca6*), cytoskeletal components (*Pcdh24*, *Ankrd43*, *Ccdc19*, *Dnahc7b*), and chaperones (*Suptó6h*, *Dcaf6*, *Cabc1*). Given the specialization of the stria vascularis as a transport epithelium, it is not surprising to find ion channels and metabolic genes specifically expressed by these melanoblasts. Similarly, because intermediate cells form part of a tight transport epithelium with tight junctions and extensive interdigitations with their neighboring cells, we were not surprised to find differentially expressed cytoskeletal genes. It is worth noting that our data set only reflects genes that are upregulated in intermediate cells compared with marginal and basal cells of the stria vascularis. If a gene is highly expressed in all three cell types, it would be omitted from our list of differentially expressed genes. For that reason, our comparison would miss genes that are expressed throughout the stria but not in skin melanoblasts.

TABLE 1 Selected genes upregulated and downregulated in intermediate cells at P1

Rank		Mean EYFP+ (RPKM)	Fold change (EYFP+ versus EYFP−)	Adjusted p-value
Genes upregulated in intermediate cells				
1	Gpr143	5,959.836833	1902.666206	5.80E−280
3	Tyrp1	3,664.97936	1755.056196	3.93E−272
5	Cck	1,493.506172	1,430.396738	7.00E−112
6	Tyr	182,803.9377	1,182.968881	< 1.0E−307
7	Tspan10	14,703.25944	1,173.496676	< 1.0E−307
8	Dct	1,229,760.603	1,040.455807	< 1.0E−307
12	Pax3	13,548.05622	810.9731896	< 1.0E−307
13	Trpm1	143,576.0942	776.8879007	< 1.0E−307
18	Foxd3	1,384.309952	662.907351	2.27E−130
20	Mlana	16,046.93495	614.7542966	2.90E−211
22	Gsta1	4,385.944061	600.0874411	6.00E−297
24	Cdh19	6,689.470212	582.4364263	6.94E−140
25	Slc45a2	80,163.93702	572.9592421	8.56E−167
28	Hpse	81,968.26535	516.4777847	7.06E−229
34	Kcnj10	20,291.84593	323.9065984	< 1.0E−307
36	Mc1r	1775.336219	242.9025436	3.97E−137
38	Ednrb	252,487.068	205.4528479	< 1.0E−307
44	Slitrk1	506.7058943	161.7648618	5.17E−51
46	Slc24a5	17,714.88984	150.1445256	7.85E−138
52	Robo3	136.4725636	130.7057938	1.65E−14
Genes downregulated in intermediate cells				
1	Trem1	0.46	0.009285371	3.50E−06
2	Stfa2l1	0.465362115	0.009689083	6.41E−06
11	Acsbg2	0.969832044	0.016586624	1.15E−06
12	Sell	0.504469929	0.018582812	0.002337972
17	Ttc6	0.504469929	0.020131379	0.004151823
23	Slc4a1	2.36591839	0.022659444	1.00E−10
29	Vsx1	0.969832044	0.025104079	0.000265144
30	Opalin	1.939664089	0.026538598	1.67E−07
31	Krt83	2.831280506	0.026847943	2.03E−10
32	Ngp	2.444134018	0.028203072	1.14E−08
33	Insrr	0.969832044	0.029026591	0.001048696
36	Msx3	22.38435265	0.030670217	3.83E−62
40	Clec3a	52.80111634	0.031685437	6.56E−127
41	Nxph4	6.749716497	0.032982149	1.63E−18
44	Srrm3	15.51731271	0.033776397	2.20E−39
45	Grin2a	7.641332914	0.034198325	7.60E−20
46	Abcc12	8.806704026	0.034286865	8.65E−23
47	Slc30a10	49.8446491	0.034368912	2.20E−109
49	Clca5	8.611164958	0.035094862	2.45E−58
50	Lingo3	7.797764168	0.03643055	1.61E−21

Note: List of 20 selected genes picked from the 50 genes showing the greatest fold change enrichment in intermediate cells in comparison with the other cells of the stria vascularis at P1. The table presents a ranking, reads per kilobase million of transcripts (RPKM), fold change in intermediate cells versus the other cells population of the stria vascularis, and the adjusted *p*-value for the difference between those populations of cells. Ranking is based on the fold change.

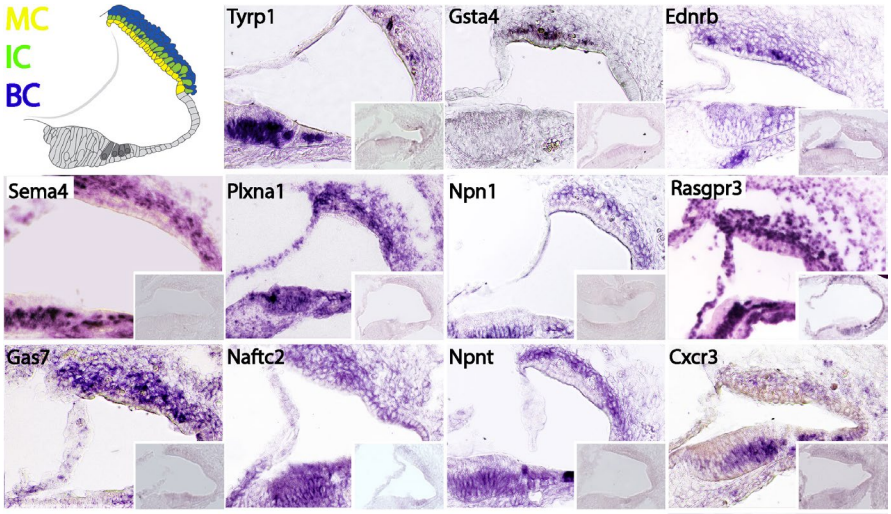

FIGURE 2 In situ validation of the RNAseq screen. The schematic shows a section through a P1 cochlea and the different layers of the stria vascularis are labeled. Expression of selected genes on cochlear section of cochlea at P1 by in situ hybridization. Inset shows negative control in situ hybridizations using sense probes. MC: marginal cells, IC: intermediate cells BC: basal cells

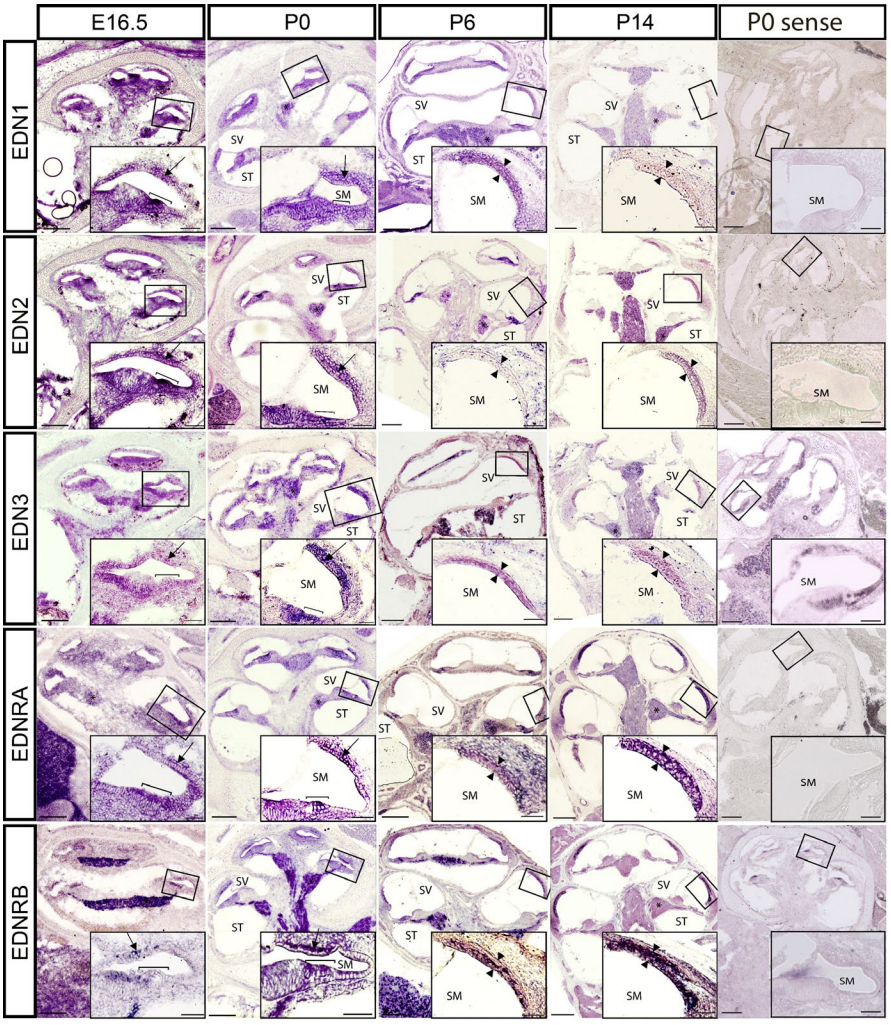

FIGURE 3 Expression of the endothelin family from E16.5 to P14 in the mouse cochlea. The gene expression of *Et-1*, *Et-2*, *Et-3*, *EdnrA*, and *EdnrB* was analyzed by in situ hybridization. Inset shows a higher magnification of the selected area. At E16.5 and P0, detail of the cochlear turn and P6-P14 detail of the stria vascularis. P0 sense column shows in situ hybridizations done with sense probes as negative controls. Square bracket: organ of corti, arrows: melanoblasts migrating in the stria vascularis, arrowheads: stria vascularis, stars: spiral ganglion. Scale bar: 200 μm, inset scale bar: 50 μm

3.4 | Developmental analysis of endothelins expression

Previous studies reported a critical window of *EdnrB* expression between E10 and E12.5 in the migratory neural crest that will give rise to melanoblasts. Disruption of *EdnrB* signaling after this period does not affect melanocyte development (Shin et al., 1999). After melanocyte differentiation, *EdnrB* is not found in healthy skin melanocytes, but it is expressed in pigmented cell lesions of the skin and increased levels of *EdnrB* are associated with malignant melanoma (Demunter et al., 2001; Lahav, 2005). In the inner ear, melanoblasts start ingressing into the lateral wall of the cochlea at around E15.5

and continue to do so until birth (Ohyama, 2017). Surprisingly, our RNAseq analysis of intermediate cells revealed high levels of *EdnrB* expression at P1. Although endothelin expression has been reported in the adult cochlea (Fujimura et al., 1999), the developmental expression of endothelins in the inner ear has been overlooked. We analyzed the expression patterns of the endothelin family in the inner ear during the development and differentiation of the stria vascularis.

We looked at the developing mouse cochlea between E16.5 and P14 since these stages encompass the development of the stria vascularis (Figure 3). We performed in situ hybridization for the three ligands of the endothelin family *Et-1*, *Et-2*, *and Et-3* and the two receptors of the family *EdnrA* and *EdnrB*. We observed that *Et-1* is present in spiral ganglion and otic epithelium until P6. After that stage, the expression of *Et-1* is no longer present in the cochlea. The second ligand of the endothelin family is also present in the spiral ganglion and otic epithelium until birth. After birth, *Et-2* expression can be seen in the spiral ganglion and the stria vascularis. *Et-3* expression pattern is similar to what we observed for *Et-2*. For the receptors of the endothelin family, *EdnrA* is present in the otic epithelium during the development of the cochlea. Around P6 when the three layers of the stria vascularis are distinguishable, the *EdnrA* receptor is present in the basal cell layer. At P14, the signal is present in the marginal and basal layers. This signal follows the immunolabeling of EDNRA in the adult as previously published (Meehan et al., 2016). The second receptor, *EdnrB*, is present in the spiral ganglion at E11.5 and in migrating cells over the otic epithelium. At P0, *EdnrB* expression is clearly visible in the intermediate cell layer of the stria vascularis. This expression is visible through P14. It is interesting to notice that the 3 ligands and the two receptors are expressed altogether at P0 in the stria vascularis. Later, *EdnrA* seems to be present in the basal cell layer, while *EdnrB* stays strictly express in intermediate cells. For the ligands, *Et-2* and *Et-3* remain expressed post-natally throughout the stria vascularis, except in the marginal cells.

Our data indicate a specific expression of the endothelin family in the stria vascularis, with a specificity of the *EdnrB* in intermediate cells at every stage of stria development, from the migrating neural crest cells to the mature epithelium.

3.5 | *EDNRB* expression suggests differences in skin versus inner ear melanocytes

Because there are no reports of *EdrnB* expression in normal skin melanocytes after they arrive in the epidermis, we were surprised to observe *EdnrB* expression persisting days and weeks after migration of the melanoblasts into the stria vascularis. This suggests that *EdnrB* may have additional functions in the inner ear relative to the skin; it is also possible, however, that instead of additional roles the timing and regulation of the pathway differ between inner ear and skin. To compare the expression of *EdnrB* between the two related cell types, we used a semi-quantitative RNAscope approach to determine the level of expression of *EdnrB* in the two different cell types during the development of the mouse (Figure 4a).

The endothelin family is transiently required for melanoblast development between E10.5 and E12.5, which corresponds to the determination of the melanocytic lineage (Luciani et al., 2011). The first stage we analyzed is E11.5, when neural crest cells are migrating through the embryo. During embryogenesis, around E13.5, the neural crest that will give rise to melanoblasts migrates and proliferates in the epidermis of the entire body. During the morphogenesis of the hair follicle, melanoblasts enter the developing hair follicle and differentiate into melanocytes (Li, 2014; Osawa, 2008) (Figure 4b).

Our quantitative analysis of *EdnrB* expression in the melanocytes of the skin and the melanoblasts of the stria vascularis showed a high level of expression during migration and differentiation of neural crest cells, with a rapid decrease in *EdnrB* expression in the mature melanoblasts of the skin, which is not seen in the melanoblasts of the ear (Figure 4c).

At E16.5 and P0, expression levels of *EdnrB* are still similar between the two cell types. After birth, melanoblasts of the skin start to decrease their expression of *EdnrB*. In the ear, a high expression level is maintained at least until P15. We suggest that the small amount of *EdnrB* mRNA at 3 months might be caused by the loss of mRNA during the decalcification process. Indeed, a prolonged treatment in EDTA may affect the preservation of the RNA. Unfortunately, at the adult stage, the cochlea is completely ossified and decalcification is necessary in order to cut a section in the stria vascularis. The number of dots present in the positive control of the ear at adult stage is low too, which could increase the difference after normalization. From single-cell RNAseq analysis in the stria vascularis, we know that the levels of *EdnrB* in intermediate cells are still elevated at P30 (Korrapati et al., 2019). We did not encounter this problem with the skin samples as the skin does not need a decalcification step and the positive control is normal compared with the other stages. We can conclude that the levels of *EdnrB* decrease drastically after birth in the skin but are maintained in the intermediate cells of the stria.

4 | DISCUSSION

In the inner ear, the neural crest cells give rise to the glia of the cochleovestibular ganglion and to two different melanocytic cell types: the pigmented cells of the vestibular system and the intermediate cells of the stria vascularis. These melanocyte-like cells are responsible for the generation of endolymph, a very unique fluid that fills the scala media and provides the energy for the mechanosensory hair cells to transduce sound into action potentials. Like skin melanocytes, these cells are absent in mutations that affect neural crest cell migration or differentiation, causing not only pigmentation defects, but also sensorineural hearing loss.

We have investigated the transcriptome of the intermediate cells of the stria vascularis at post-natal day 1, after they have ingressed in

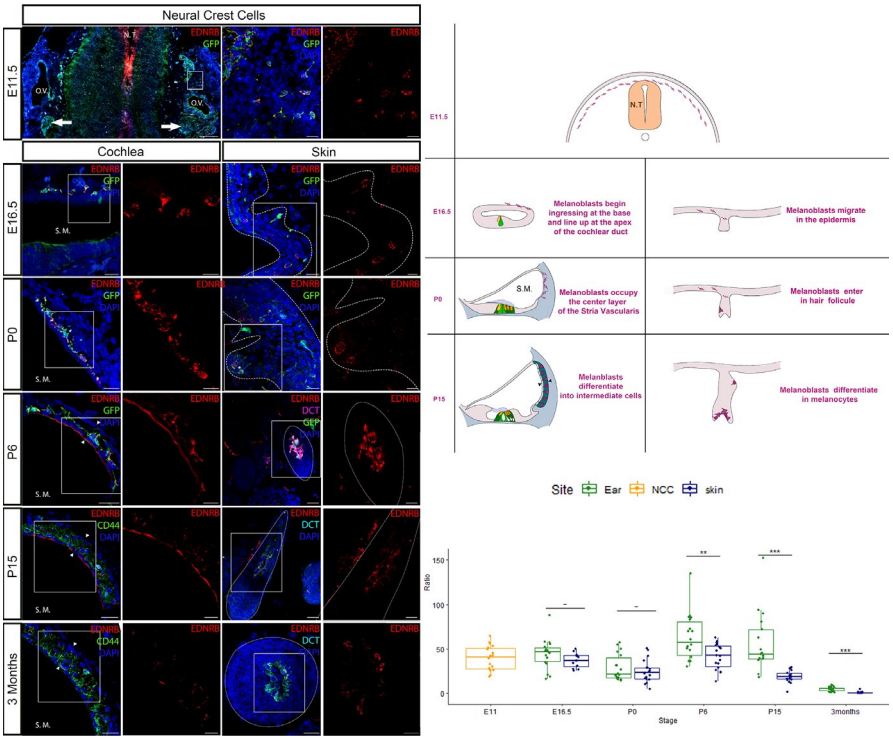

FIGURE 4 Semi-quantitative analysis of the endothelin receptor B expression shows a difference in *EdnrB* regulation between the melanocytes of the skin and the melanocytes of the ear at post-natal stages. a: RNAscope of *EdnrB* (red) with immunolocalization of melanocytes using DCT (turquoise or purple) and neural crest cell derivatives using GFP expression in Wnt1Cre-EYFP mice (green). Nucleus are labeled in blue by DAPI. Arrowheads mark the stria vascularis thickness, and arrows indicate the spiral ganglion containing glial cells originating from neural crest cells. Dashed lines mark the epidermis, dotted lines mark the hair follicle, and the star indicates the hair follicle in formation. NT: neural tube, OV: otic vesicle, SM: scala media. E11.5 panel, general scale bar: 200 μm, inset scale bar: 20 μm. All other panels, general scale bar: 20 μm, inset scale bar: 10 μm. Note: the transverse section in 3 months hair follicles is through the differentiated melanocytes only. b: Schematic representation of melanocytic cells development in the cochlea and skin. c: After the RNAscope assay was performed, the average mRNA expression was quantified by dividing the total spot count by the number of cells count per section. 3 animals were used for each stage (except E16.5 skin (2)). *=$p < 0.05$ based on the Kruskal–Wallis test

the lateral wall of the cochlea, but before they are fully differentiated and the stria vascularis reaches functional and morphological maturity. The association between Wnt1Cre-EYFP mice and Fluorescent Activated Cell Sorting (FACS) tools allowed us to isolate the melanoblasts of the stria vascularis and compare their transcriptome with that of the remaining cell types of this complex epithelium and with skin melanoblasts. From our RNAseq analysis, we found that intermediate cells are highly enriched in genes specific for melanocytic lineage and differentiation, such as *Tyrp1*, *Tyr*, *Mitf*, *Dct*, and *Slc45a2*, which imply that these cells already start their differentiation at or before P1. Surprisingly, we also found genes known to be antagonists of melanocytic differentiation such as *FoxD3*. *FoxD3* controls the lineage choice between neural–glial and pigment cells by repressing MITF during the early phase of neural crest migration (Thomas & Erickson, 2009). In addition, we found that neonatal intermediate cells are also highly enriched for undifferentiated neural crest genes such as *Pax3*, *Tcfap2a*, *and Sox10*. This last group is interesting as it shows that the melanoblast present at P0 is still in a transient stage between glial and intermediate cell fate. Our results support recent research showing that non-cutaneous melanocytes, such as intermediate cells, arise from Schwann cells precursor-derived melanocytes, which express *Plp1*, *Dhh*, and *Sox10* (Adameyko et al., 2009, 2012; Deo et al., 2013) Also enriched in intermediate cells are neural crest and axon guidance ligand–receptor pairs such as neuropilins/plexins and Robo/slit. ROBO3 has been mostly shown for its role in axon guidance, but the receptor–ligand Robo/Slit interaction is also present in melanoblasts, where its potential role for repulsion has been proposed to guide the proper dispersion of the melanoblast in the skin (Laurent-Gengoux et al., 2018).

When compared to E17.5 skin, we found that there are at least 266 transcripts present P1 in intermediate cells but not in skin melanoblasts. These transcripts likely reflect functional specializations of pigmented cells in the stria vascularis. In fact, many of these genes are ion channels, as expected in a transport epithelium. Other genes present in intermediate cells are cytoskeletal components, which may also reflect the different architecture of intermediate cells in a tight epithelium specialized in potassium transport when compared to skin melanocytes. Metabolic genes such as interferon receptors and interferon downstream proteins that could play a role in the stria vascularis response in pathologies such as Meniere's disease are also differentially expressed in inner ear melanoblasts but not in skin.

An embryonic mutation in the endothelin receptor B causes piebaldism in mice and the Waardenburg syndrome in humans. Affected individuals have an aganglionic megacolon, pigmentation abnormalities, heterochromia, and hearing loss. This phenotype is also caused by mutations in endothelin 3 in the same cells, which argues for autocrine signaling. Interestingly, ET-1 in the marginal cells of the stria has been shown to act through *EdnrA* in a paracrine manner and through *EdnrB* in adult cochleas.

EdnrB is only necessary for neural crest migration during a short embryonic window of time, between E10.5 and E12.5 in mice. In vivo, *EdnrB* seems to be dispensable for skin melanocyte differentiation once the melanoblasts arrive in the hair follicles. But a conditional knockout of *Ednrb* in adult mice displayed hair-greying phenotype. Several studies on physiological and epilation-induced hair regeneration showed that EDN/EDNRB signaling promotes proliferation and differentiation of melanocyte stem cells present in the hair follicles (Chang et al., 2013; Li et al., 2017; Takeo et al., 2016).

Previous research indicates that the endothelin signaling is still used to regulate the melanocytes in the dermis but not the epidermis after embryogenesis. For example, a hypermorphic mutation in *Gnaq* or *Gna11*, two G protein downstream effectors of EDNRB, leads to a dermal but not an epidermal hyperpigmentation (Van Raamsdonk et al., 2004). It has also been shown that the overexpression of *Edn3* in keratinocytes leads to hyperpigmentation of the dermis but not the epidermis. Moreover, when the overexpression of *Edn3* stops, this hyperpigmentation is not maintained (Garcia et al., 2008). Finally, Van Raamsdonk and her team showed that endothelin/Gαq pathway regulates melanocyte numbers and pigment quantity independently in the hair follicles (Van Raamsdonk et al., 2009). In parallel, the regional requirement for Ednrb was speculated to be related to environmental differences or differences in the origin of the melanoblasts themselves as some arise from the Schwann cell precursors associated with cranial nerves (Deo et al., 2013).

Upregulation of *EdnrB* in skin melanocytes is commonly associated with melanoma proliferation (Saldana-Caboverde & Kos, 2010) and endothelin signaling as an important regulator of tumorigenesis in non-epithelial melanomas (Jain et al., 2020). In a mutant mouse expressing an oncogenic G protein GNAQ, the central nervous system and the inner ear present melanocytic hyperplasia (Huang et al., 2015). Interestingly, while the melanocytes present in the stria vascularis are considered non-cutaneous melanocytes, no melanoma of the ear is known so far to originate from the intermediate cells. A case of melanoma in the cochlea was reported in 2014, but the melanocytes were originating from the melanocytes of the nervous system, which could be the case in the oncogenic GNAQ model (Koshy et al., 2014).

The role (or roles) of *EdnrB* during inner ear development and the onset of hearing have not been fully studied beyond syndromic deafness in the embryonic mutants. This has been in part due to the early lethality of *EdnrB*$^{-/-}$ pups, which die around the time of hearing onset. In addition, *EdnrB* is not only expressed in intermediate cells of the stria vascularis, but also expressed in the glial cells of the VIII ganglion, where it seems to have an important role in hearing (Ida-Eto et al., 2011).

Our results show a sustained expression of *EdnrB* in intermediate cells of the stria from embryonic development through at least three months after birth. This is a critical period during the development, differentiation, and maturation of intermediate cells. During this time, neural crest cell precursors migrate into the lateral wall of the cochlea, and they integrate into their final position between marginal cells and basal cells of the stria, and undergo dramatic morphological and functional changes. These include proliferation, acquisition of a cylindrical shape, formation of extensive interdigitations that form tight junctions with other cell types, and close association with capillary vessels that invade the stria from the spiral ligament plexus. Our data suggest that endothelin signaling may be mediating one or several of these processes. In addition to endothelin-3, we also observed the presence of the other ligands in the family and *EdnrA*. *Endothelin-1*, which is expressed in the adult stria, has been implicated in the early onset of strial presbycusis (Uchida et al., 2009, 2013).

From previous studies, we know that skin and inner ear melanocytes contain several transcriptomic differences (Uehara et al., 2009). Our data identified many more transcriptional differences and also suggest that these cell types might also differ in their regulation of endothelin signaling, with skin melanocytes rapidly downregulating *EdnrB* expression after birth, while intermediate cells maintain high levels of expression until at least P90. It is tempting to speculate that functional differences between skin and stria melanocytic cells, and even between vestibular and cochlear melanocytes, may have arisen during evolution when pigmented cells were co-opted as part of the cochlear transport epithelium. In birds, the generation of endolymph and endocochlear potential is carried by the tegmentum vasculosum, the homologue of the stria vascularis. However, this epithelium consists of a single layer of cells that are homologous to the marginal cells of the lateral wall (Wilms et al., 2016). Intermediate cells, in contrast to skin melanocytes, express the K^+ channel Kir.4 (Hibino et al., 2010), as do marginal and basal cells. This is another example of melanocytic cell divergence that could account for new roles of endothelins during intermediate cell development.

Our analysis of the neonatal transcriptome of intermediate cells confirms the presence of the endothelin family during the development of the stria vascularis. We showed that melanoblasts present at P1 in the cochlea are still in a transient stage between migratory neural crest, glial, and intermediate cells fate. We also show the sustained expression of *EdnrB* at different relevant developmental stages such as neural crest cell migration, ingression in the lateral wall of the cochlea, differentiation of intermediate cells, and angiogenesis in the stria vascularis. Our data suggest differences in the regulation of *EdnrB* expression between skin and cochlear melanocytes, which could represent evolutionary divergence of pigmented cells. These findings set a framework for further studies that will allow us to understand the functional

significance of the transcriptomic differences between inner ear and skin melanoblasts as well as the different roles that the endothelin family and more specifically *EdnrB* play in the intermediate cell and stria vascularis development.

ACKNOWLEDGEMENTS

We would like to thank Ying-Wooi Wan from the Baylor College of Medicine Bioinformatics Core for assistance with RNAseq analysis, Dr. Maxwell Lee and Dr. Glenn Merlino from NIH for sharing their E17.5 melanoblast transcriptome data set, Dr. Radhika Atit for helpful assistance with skin histology, and Dr. Andrew Groves for helpful comments on the manuscript. This work was funded by an Emerging Research Grant from HHF to MLB and by NIH/NIDCD 1 R01 DC015785-01 to MLB.

ORCID

Justine M. Renauld https://orcid.org/0000-0003-4759-4021
Martin L. Basch https://orcid.org/0000-0002-3156-5376

REFERENCES

Adameyko, I., Lallemend, F., Aquino, J. B., Pereira, J. A., Topilko, P., Müller, T., … Ernfors, P. (2009). Schwann cell precursors from nerve innervation are a cellular origin of melanocytes in skin. *Cell*, *139*(2), 366–379. https://doi.org/10.1016/j.cell.2009.07.049

Adameyko, I., Lallemend, F., Furlan, A., Zinin, N., Aranda, S., Kitambi, S. S., … Ernfors, P. (2012). Sox2 and Mitf cross-regulatory interactions consolidate progenitor and melanocyte lineages in the cranial neural crest. *Development*, *139*(2), 397–410. https://doi.org/10.1242/dev.065581

Ali, S. A., & Naaz, I. (2015). Current Challenges in Understanding the Story of Skin Pigmentation — Bridging the Morpho-Anatomical and Functional Aspects of Mammalian Melanocytes. In Muscle Cell and Tissue.

Aoki, H., Yamada, Y., Hara, A., & Kunisada, T. (2009). Two distinct types of mouse melanocyte: Differential signaling requirement for the maintenance of non-cutaneous and dermal versus epidermal melanocytes. *Development*, *136*(15), 2511–2521. https://doi.org/10.1242/dev.037168

Basch, M. L., & Bronner-Fraser, M. (2006). Neural crest inducing signals. *Advances in Experimental Medicine and Biology*, *589*, 24–31.

Baynash, A. G., Hosoda, K., Giaid, A., Richardson, J. A., Emoto, N., Hammer, R. E., & Yanagisawa, M. (1994). Interaction of endothelin-3 with endothelin-B receptor is essential for development of epidermal melanocytes and enteric neurons. *Cell*, *79*(7), 1277–1285. https://doi.org/10.1016/0092-8674(94)90018-3

Cable, J., Barkway, C., & Steel, K. P. (1992). Characteristics of stria vascularis melanocytes of viable dominant spotting (Wv/Wv) mouse mutants. *Hearing Research*, *64*(1), 6–20.

Cai, T., Jen, H. I., Kang, H., Klisch, T. J., Zoghbi, H. Y., & Groves, A. K. (2015). Characterization of the transcriptome of nascent hair cells and identification of direct targets of the Atoh1 transcription factor. *Journal of Neuroscience*, *35*(14), 5870–5883. https://doi.org/10.1523/JNEUROSCI.5083-14.2015

Casale, J., & Agarwal, A. (2020). *Anatomy, Head and Neck*. Ear Endolymph. In StatPearls.

Chang, C. Y., Pasolli, H. A., Giannopoulou, E. G., Guasch, G., Gronostajski, R. M., Elemento, O., & Fuchs, E. (2013). NFIB is a governor of epithelial-melanocyte stem cell behaviour in a shared niche. *Nature*, *495*(7439), 98–102. https://doi.org/10.1038/nature11847

Davenport, A. P., Hyndman, K. A., Dhaun, N., Southan, C., Kohan, D. E., Pollock, J. S., Pollock, D. M., Webb, D. J., & Maguire, J. J. (2016). Endothelin. *Pharmacological Reviews*, *68*(2), 357–418. https://doi.org/10.1124/pr.115.011833

Demunter, A., De Wolf-Peeters, C., Degreef, H., & Stas, M. (2001). Expression of the endothelin-B receptor in pigment cell lesions of the skin. Evidence for its role as tumor progression marker in malignant melanoma. *Virchows Archiv*, *438*(5), 485–491. https://doi.org/10.1007/s004280000362

Deo, M., Huang, J. L., & Van Raamsdonk, C. D. (2013). Genetic interactions between neurofibromin and endothelin receptor B in mice. *PLoS One*, *8*(3), e59931. https://doi.org/10.1371/journal.pone.0059931

Djian-Zaouche, J., Campagne, C., Reyes-Gomez, E., Gadin-Czerw, S., Bernex, F., Louise, A., … Aubin-Houzelstein, G. (2012). Pax3 (GFP), a new reporter for the melanocyte lineage, highlights novel aspects of PAX3 expression in the skin. *Pigment Cell & Melanoma Research*, *25*(5), 545–554. https://doi.org/10.1111/j.1755-148X.2012.01024.x

Druckenbrod, N. R., Powers, P. A., Bartley, C. R., Walker, J. W., & Epstein, M. L. (2008). Targeting of endothelin receptor-B to the neural crest. *Genesis*, *46*(8), 396–400. https://doi.org/10.1002/dvg.20415

Fitch, K. R., McGowan, K. A., van Raamsdonk, C. D., Fuchs, H., Lee, D., Puech, A., & Barsh, G. S. (2003). Genetics of dark skin in mice. *Genes & Development*, *17*(2), 214–228. https://doi.org/10.1101/gad.1023703

Fujimura, T., Furukawa, H., Doi, Y., Makishima, K., & Fujimoto, S. (1999). Immunoreactivity of endothelins and endothelin receptor in the stria vascularis of the mouse cochlea. *Hearing Research*, *128*(1–2), 135–146. https://doi.org/10.1016/S0378-5955(98)00206-8

Furlan, A., & Adameyko, I. (2018). Schwann cell precursor: A neural crest cell in disguise? *Developmental Biology*, *444*(Suppl 1), S25–S35. https://doi.org/10.1016/j.ydbio.2018.02.008

Garcia, R. J., Ittah, A., Mirabal, S., Figueroa, J., Lopez, L., Glick, A. B., & Kos, L. (2008). Endothelin 3 induces skin pigmentation in a keratin-driven inducible mouse model. *The Journal of Investigative Dermatology*, *128*(1), 131–142. https://doi.org/10.1038/sj.jid.5700948

Hibino, H., Nin, F., Tsuzuki, C., & Kurachi, Y. (2010). How is the highly positive endocochlear potential formed? The specific architecture of the stria vascularis and the roles of the ion-transport apparatus. *Pflugers Archiv - European Journal of Physiology*, *459*(4), 521–533. https://doi.org/10.1007/s00424-009-0754-z

Hosoda, K., Hammer, R. E., Richardson, J. A., Baynash, A. G., Cheung, J. C., Giaid, A., & Yanagisawa, M. (1994). Targeted and natural (piebald-lethal) mutations of endothelin-B receptor gene produce megacolon associated with spotted coat color in mice. *Cell*, *79*(7), 1267–1276. https://doi.org/10.1016/0092-8674(94)90017-5

Huang, J. L., Urtatiz, O., & Van Raamsdonk, C. D. (2015). Oncogenic G protein GNAQ induces uveal melanoma and intravasation in mice. *Cancer Research*, *75*(16), 3384–3397. https://doi.org/10.1158/0008-5472.CAN-14-3229

Ida-Eto, M., Ohgami, N., Iida, M., Yajima, I., Kumasaka, M. Y., Takaiwa, K., … Kato, M. (2011). Partial requirement of endothelin receptor B in spiral ganglion neurons for postnatal development of hearing. *Journal of Biological Chemistry*, *286*(34), 29621–29626. https://doi.org/10.1074/jbc.M111.236802

Jain, F., Longakit, A., Huang, J. L., & Van Raamsdonk, C. D. (2020). Endothelin signaling promotes melanoma tumorigenesis driven by constitutively active GNAQ. *Pigment Cell & Melanoma Research*, *33*(6), 834–849. https://doi.org/10.1111/pcmr.12900

Korrapati, S., Taukulis, I., Olszewski, R., Pyle, M., Gu, S., Singh, R., … Hoa, M. (2019). Single cell and single nucleus RNA-Seq reveal cellular heterogeneity and homeostatic regulatory networks in adult mouse stria vascularis. *Frontiers in Molecular Neuroscience*, *12*, 316. https://doi.org/10.3389/fnmol.2019.00316

Koshy, A. N., Briggs, R. J., & Dally, M. (2014). Primary melanoma of the cochlea with cerebellopontine extension and leptomeningeal spread.

Journal of Laryngology and Otology, *128*(Suppl 2), S59–62. https://doi.org/10.1017/S002221511400019X

Lahav, R. (2005). Endothelin receptor B is required for the expansion of melanocyte precursors and malignant melanoma. *International Journal of Developmental Biology*, *49*(2–3), 173–180. https://doi.org/10.1387/ijdb.041951rl

Laurent-Gengoux, P., Petit, V., Aktary, Z., Gallagher, S., Tweedy, L., Machesky, L., & Larue, L. (2018). Simulation of melanoblast displacements reveals new features of developmental migration. *Development*, *145*(12), dev160200. https://doi.org/10.1242/dev.160200

Lee, H.-O., Levorse, J. M., & Shin, M. K. (2003). The endothelin receptor-B is required for the migration of neural crest-derived melanocyte and enteric neuron precursors. *Developmental Biology*, *259*(1), 162–175. https://doi.org/10.1016/s0012-1606(03)00160-x

Lewis, A. E., Vasudevan, H. N., O'Neill, A. K., Soriano, P., & Bush, J. O. (2013). The widely used Wnt1-Cre transgene causes developmental phenotypes by ectopic activation of Wnt signaling. *Developmental Biology*, *379*(2), 229–234. https://doi.org/10.1016/j.ydbio.2013.04.026

Li, A. (2014). The biology of melanocyte and melanocyte stem cell. *Acta Biochimica Et Biophysica Sinica*, *46*(4), 255–260. https://doi.org/10.1093/abbs/gmt145

Li, H., Fan, L., Zhu, S., Shin, M. K., Lu, F., Qu, J., & Hou, L. (2017). Epilation induces hair and skin pigmentation through an EDN3/EDNRB-dependent regenerative response of melanocyte stem cells. *Scientific Reports*, *7*(1), 7272. https://doi.org/10.1038/s41598-017-07683-x

Luciani, F., Champeval, D., Herbette, A., Denat, L., Aylaj, B., Martinozzi, S., … Delmas, V. (2011). Biological and mathematical modeling of melanocyte development. *Development*, *138*(18), 3943–3954. https://doi.org/10.1242/dev.067447

Maass, J. C., Gu, R., Cai, T., Wan, Y.-W., Cantellano, S. C., Asprer, J. S. T., … Groves, A. K. (2016). Transcriptomic analysis of mouse cochlear supporting cell maturation reveals large-scale changes in notch responsiveness prior to the onset of hearing. *PLoS One*, *11*(12), e0167286. https://doi.org/10.1371/journal.pone.0167286

Maguire, J. J., & Davenport, A. P. (2015). Endothelin receptors and their antagonists. *Seminars in Nephrology*, *35*(2), 125–136. https://doi.org/10.1016/j.semnephrol.2015.02.002

Marie, K. L., Sassano, A., Yang, H. H., Michalowski, A. M., Michael, H. T., Guo, T., … Mishra, P. J. (2020). Melanoblast transcriptome analysis reveals pathways promoting melanoma metastasis. *Nature Communications*, *11*(1), 333. https://doi.org/10.1038/s41467-019-14085-2

Matsushima, Y., Shinkai, Y., Kobayashi, Y., Sakamoto, M., Kunieda, T., & Tachibana, M. (2014). A mouse model of Waardenburg syndrome type 4 with a new spontaneous mutation of the endothelin-B receptor gene. *Mammalian Genome*, *13*(1), 30–35. https://doi.org/10.1007/s00335-001-3038-2

Meehan, D. T., Delimont, D., Dufek, B., Zallocchi, M., Phillips, G., Gratton, M. A., & Cosgrove, D. (2016). Endothelin-1 mediated induction of extracellular matrix genes in strial marginal cells underlies strial pathology in Alport mice. *Hearing Research*, *341*, 100–108. https://doi.org/10.1016/j.heares.2016.08.003

Ni, C., Zhang, D., Beyer, L. A., Halsey, K. E., Fukui, H., Raphael, Y., & Hornyak, T. J. (2013). Hearing dysfunction in heterozygous Mitf(Mi-wh) /+ mice, a model for Waardenburg syndrome type 2 and Tietz syndrome. *Pigment Cell Melanoma Research*, *26*(1), 78–87. https://doi.org/10.1111/pcmr.12030

Nin, F., Yoshida, T., Sawamura, S., Ogata, G., Ota, T., Higuchi, T., … Hibino, H. (2016). The unique electrical properties in an extracellular fluid of the mammalian cochlea; their functional roles, homeostatic processes, and pathological significance. *European Journal of Physiology*, *468*(10), 1637–1649. https://doi.org/10.1007/s00424-016-1871-0

Ohyama, T. (2017). There's no place like home - HGF-c-MET signaling and melanocyte migration into the mammalian cochlea. *Neurogenesis*, *5*(1), https://doi.org/10.1080/23262133.2017.1317693

Osawa, M. (2008). Melanocyte stem cells. *StemBook*.

Prasad, M. S., Charney, R. M., & Garcia-Castro, M. I. (2019). Specification and formation of the neural crest: Perspectives on lineage segregation. *Genesis*, *57*(1), e23276. https://doi.org/10.1002/dvg.23276

Sakurai, T., Yanagisawa, M., Takuwa, Y., Miyazaki, H., Kimura, S., Goto, K., & Masaki, T. (1990). Cloning of a cDNA encoding a non-isopeptide-selective subtype of the endothelin receptor. *Nature*, *348*(6303), 732–735. https://doi.org/10.1038/348732a0

Saldana-Caboverde, A., & Kos, L. (2010). Roles of endothelin signaling in melanocyte development and melanoma. *Pigment Cell Melanoma Res*, *23*(2), 160–170. https://doi.org/10.1111/j.1755-148X.2010.00678.x

Shi, X. R. (2016). Pathophysiology of the cochlear intrastrial fluid-blood barrier (review). *Hearing Research*, *338*, 52–63. https://doi.org/10.1016/j.heares.2016.01.010

Shibata, S., Miwa, T., Wu, H. H., Levitt, P., & Ohyama, T. (2016). Hepatocyte growth factor-c-MET signaling mediates the development of non-sensory structures of the mammalian cochlea and hearing. *Journal of Neuroscience*, *36*(31), 8200–8209. https://doi.org/10.1523/JNEUROSCI.4410-15.2016

Shin, M. K., Levorse, J. M., Ingram, R. S., & Tilghman, S. M. (1999). The temporal requirement for endothelin receptor-B signalling during neural crest development. *Nature*, *402*(6761), 496–501. https://doi.org/10.1038/990040

Steel, K. P., & Barkway, C. (1989). Another role for melanocytes: Their importance for normal stria vascularis development in the mammalian inner ear. *Development*, *107*(3), 453–463.

Stern, C. D. (1998). Detection of multiple gene products simultaneously by in situ hybridization and immunohistochemistry in whole mounts of avian embryos. *Curr Top Dev Biol*, *36*, 223–243.

Tachibana, M., Kobayashi, Y., & Matsushima, Y. (2003). Mouse models for four types of Waardenburg syndrome. *Pigment Cell Research*, *16*(5), 448–454. https://doi.org/10.1034/j.1600-0749.2003.00066.x

Takeo, M., Lee, W., Rabbani, P., Sun, Q. I., Hu, H., Lim, C. H., Manga, P., & Ito, M. (2016). EdnrB governs regenerative response of melanocyte stem cells by crosstalk with Wnt signaling. *Cell Reports*, *15*(6), 1291–1302. https://doi.org/10.1016/j.celrep.2016.04.006

Tharmarajah, G., Eckhard, U., Jain, F., Marino, G., Prudova, A., Urtatiz, O., … Van Raamsdonk, C. D. (2018). Melanocyte development in the mouse tail epidermis requires the Adamts9 metalloproteinase. *Pigment Cell & Melanoma Research*, *31*(6), 693–707. https://doi.org/10.1111/pcmr.12711

Thomas, A. J., & Erickson, C. A. (2009). FOXD3 regulates the lineage switch between neural crest-derived glial cells and pigment cells by repressing MITF through a non-canonical mechanism. *Development*, *136*(11), 1849–1858. https://doi.org/10.1242/dev.031989

Uchida, Y., Sugiura, S., Nakashima, T., Ando, F., & Shimokata, H. (2009). Endothelin-1 gene polymorphism and hearing impairment in elderly Japanese. *Laryngoscope*, *119*(5), 938–943. https://doi.org/10.1002/lary.20181

Uchida, Y., Teranishi, M., Nishio, N., Sugiura, S., Hiramatsu, M., Suzuki, H., … Nakashima, T. (2013). Endothelin-1 gene polymorphism in sudden sensorineural hearing loss. *Laryngoscope*, *123*(11), E59–65. https://doi.org/10.1002/lary.24298

Uehara, S., Izumi, Y., Kubo, Y., Wang, C. C., Mineta, K., Ikeo, K., & Yamamoto, H. (2009). Specific expression of Gsta4 in mouse cochlear melanocytes: A novel role for hearing and melanocyte differentiation. *Pigment Cell & Melanoma Research*, *22*(1), 111–119.

Van Raamsdonk, C. D., Barsh, G. S., Wakamatsu, K., & Ito, S. (2009). Independent regulation of hair and skin color by two G protein-coupled pathways. *Pigment Cell & Melanoma Research*, *22*(6), 819–826. https://doi.org/10.1111/j.1755-148X.2009.00609.x

Van Raamsdonk, C. D., Fitch, K. R., Fuchs, H., de Angelis, M. H., & Barsh, G. S. (2004). Effects of G-protein mutations on skin color. *Nature Genetics*, *36*(9), 961–968. https://doi.org/10.1038/ng1412

Vandamme, N., & Berx, G. (2019). From neural crest cells to melanocytes: Cellular plasticity during development and beyond. *Cellular and*

Molecular Life Sciences, *76*(10), 1919–1934. https://doi.org/10.1007/s00018-019-03049-w

Waardenburg, P. J. (1951). A new syndrome combining developmental anomalies of the eyelids, eyebrows and nose root with pigmentary defects of the iris and head hair and with congenital deafness. *American Journal of Human Genetics*, *3*(3), 195–253.

Wilms, V., Koppl, C., Soffgen, C., Hartmann, A. M., & Nothwang, H. G. (2016). Molecular bases of K(+) secretory cells in the inner ear: Shared and distinct features between birds and mammals. *Scientific Reports*, *6*, 34203. https://doi.org/10.1038/srep34203

Yoshida, H., Kunisada, T., Kusakabe, M., Nishikawa, S., & Nishikawa, S. I. (1996). Distinct stages of melanocyte differentiation revealed by analysis of nonuniform pigmentation patterns. *Development*, *122*(4), 1207–1214.

SUPPORTING INFORMATION

Additional supporting information may be found online in the Supporting Information section.

How to cite this article: Renauld JM, Davis W, Cai T, Cabrera C, Basch ML. Transcriptomic analysis and *ednrb* expression in cochlear intermediate cells reveal developmental differences between inner ear and skin melanocytes. *Pigment Cell Melanoma Res*. 2021;34:585–597. https://doi.org/10.1111/pcmr.12961